An L-Band Leaky-Wave Array Antenna for High Power Microwave Applications

Shaofeng Bi, *Graduate Student Member, IEEE*, Chengwei Yuan, Qiang Zhang, and Yunfei Sun

***Abstract*—This work seeks a novel design for a compact leaky-wave array antenna for high-power microwave (HPM) applications. The leaky-wave antenna is made of a rectangular waveguide with closely spaced non-resonant slots in the broad-wall of the waveguide. By this means, more slots can be set within a unit length and less energy will radiate from each slot, then higher power-handling capacity can be achieved. An L-band leaky-wave waveguide antenna centered at 1.57 GHz is designed and experimentally studied. The results show that the radiation efficiency of the antenna is 97% and the power-handling capacity of a single waveguide exceeds 1.3 GW. In addition, a 5-waveguide array antenna is also designed. The antenna array has an aperture efficiency of 76.6% and the beam scanning range can reach ±40° in H-plane, which would be suitable for many HPM applications.**

***Index Terms*—Leaky-wave antenna, high-power microwave (HPM), beam scanning, rectangular waveguide, non-resonant slot.**

I. INTRODUCTION

With the rapid development of high-power microwave (HPM) technology, the transmitting antenna with compact structure, high power-handling capacity and extended scanning range is urgently needed. The slotted waveguide antenna array is valued for its relatively low profile, high gain, and rugged structure, which has been employed for many decades in a wide variety of applications including wireless communications, radar, and electronically scanned arrays [1]-[3]. Recently, the slotted waveguide array has attracted interest for HPM applications due to the merits of compact, light, easy to form phased arrays as well as high power handing capacity [4]-[9]. However, when traditional technique is applied to design L-band slot antenna, the designed antenna only has a limited number of slots because the space between the slots is usually half wavelength or one wavelength. Generally, too few slots are not enough to radiate high power microwave, which could lead to a low power handing capacity. For this reason, leaky-wave array antenna (LWA) has attracted the attention of researchers and has been used to design higher power antenna arrays [10],[11]. LWAs have the advantage of high gain and compact size, and they are easier to be conformal with the carrying platform. LWAs based on ridge waveguide and stepped rectangular waveguide were also proposed for millimeter wave applications [12],[13]. In recent years, substrate integrated waveguide (SIW) leaky-wave antenna has attracted extensive attention [14]-[17]. It consists of a wide microstrip line that is shorted at the edges with conductive vias, acting as a rectangular waveguide. The slots at both ends are often tapered to suppress the reflected wave. However, the breakdown threshold of dielectric materials is very low [18], which is insufficient in HPM applications, where the output power of HPM source has reached GW class [19]. On the other hand, the slot length in high power cannot be too short in order to avoid electric field enhancement. The metal surface breakdown threshold in the vacuum state is higher than most common dielectric materials used in the microwave band [20]. In [21], Goldstone and Oliner employed a microwave network approach to describe and analyze leaky-wave antennas, which is the pioneering work of air-filled leaky-wave antenna.

In this communication, we propose an L-band leaky-wave antenna which is based on the air-filled rectangular waveguide with transverse slots in the broad-wall. The closely placed slots allow the antenna to have more slots than the traditional ones in a unit length. This is helpful to improve the power-handling capacity of the antenna. When the slotted waveguide is set as an array, the height of the array will not increase because the slots are cut in the broad-wall of the waveguide. Furthermore, when combined with the high power phase-shifters [22],[23], the antenna can steer the beam in a maximum elevation angle of 40° in H-plane with a maximum gain of 25dBi, corresponding to an aperture efficiency of 76.6%. Furthermore, the power-handling capacity of the antenna array exceeds 6.87 GW under vacuum condition.

II. BASIC STRUCTURE OF THE ANTENNA

The proposed leaky-wave array antenna is shown in Fig. 1. It is composed of five waveguides in parallel. There are groups of closely spaced transverse slots in the waveguide's broad-wall. The dimensions of the broad-wall and narrow-wall of the waveguide are a and b respectively. The width of the slot is w and the length of the slot is S. The length of the slots is shorter than resonant length [24], so they are non-resonant slots. The spacing between adjacent slots is d, which is far less than half of the wavelength. Therefore, more slots can be cut in a unit length, and both the power-handling capacity and aperture efficiency of the antenna can be improved. A dielectric plate is placed over the slots to ensure that the antenna can be pumped into a vacuum state to further increase the power-handling capacity. The dielectric plate is supported by dielectric strips, the distance between the dielectric plate and the surface of the waveguide is h.

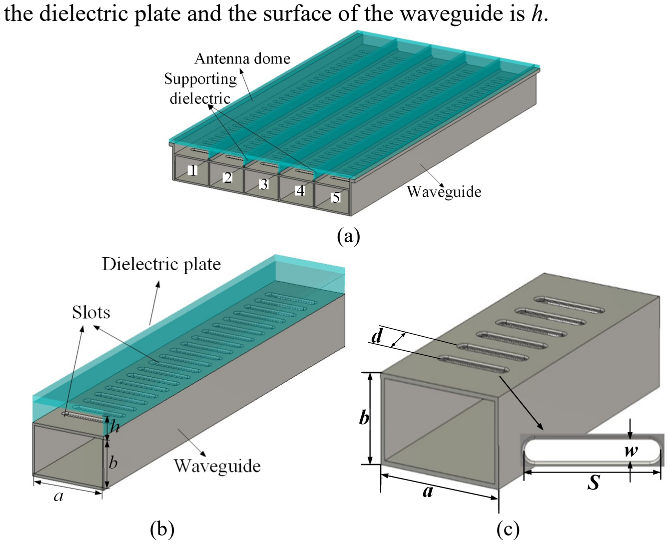

Fig. 1. Configuration of the leaky-wave array antenna. (a) The whole array. (b) Single waveguide. (c) Slots arrangement.

In this design, the length of the slot is not near the resonance length, which means that the imaginary part of the equivalent impedance of

Manuscript received July 24, 2021; revised July 25, 2022; accepted January 02, 2023. *(Shaofeng Bi and Chengwei Yuan contributed equally to this work.) (Corresponding author: Yunfei Sun.)*

The authors are with the College of Advanced Interdisciplinary Studies, National University of Defense Technology, Changsha 410073, China (e-mail: sunyunfei_gfkd@163.com)

Color versions of one or more of the figures in this communication are available online at http://ieeexplore.ieee.org.

Digital Object Identifier XXXXXXXXXXXXX

the slot cannot be ignored. As a result, there is an extra phase delay when the microwave propagates through the slot in the waveguide. Therefore, the propagation constant β of the TE_{10} mode in rectangular waveguide can be modified as

$$\beta = \frac{2\pi\sqrt{1-(\lambda/2a)^2}}{\lambda} + \frac{\Delta\phi}{d} \quad (1)$$

Where λ is the wavelength in free space and $\Delta\phi$ is the extra phase delay caused by the slot. Furthermore, the beam direction θ of the waveguide slot array is determined by

$$\theta = \arcsin(\frac{\beta\lambda}{2\pi}) \quad (2)$$

Meanwhile, there is a reflection when the wave passes through the slots. However, if we choose the interspace of each slots d to be $\lambda_g/(4n)$, where λ_g is the guided wavelength and n is an integer, the reflection phase difference of the i-th and $(i+n)$-th slots is π, as a result, the reflection will be suppressed to a certain extent.

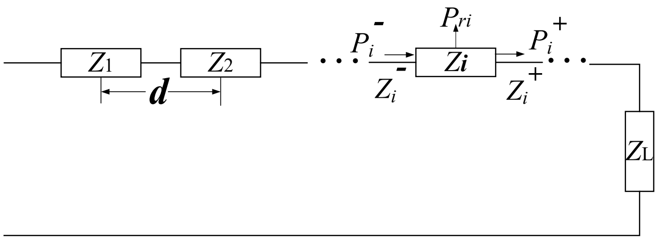

Fig. 2. The equivalent circuit of the leaky-wave antenna.

According to A. F. Stevenson's theory [25], the slots cut in the walls of a waveguide can be equivalent to a series or shunt element in a transmission line. The slot here is cut transversely in the broad-wall of the waveguide, so it can be equivalent as impedance. Fig. 2 shows the equivalent circuit of the broad-wall leaky-wave antenna. The meaning of each symbol is as follows (where the slot impedance is the equivalent impedance that includes the mutual coupling): $z_i = r_i + jx_i$, z_i, r_i, x_i are the normalized impedance, resistance, and reactance of the i-th slot, respectively. The reactance equals to zero when slots work on resonant state; $z_i^+ = r_i^+ + jx_i^+$ is the normalized impedance when look right to the load from the i-th slot; $z_i^- = r_i^- + jx_i^-$ is the normalized impedance when look left to the load from the i-th slot; P_{ri} is the radiation power of the i-th slot; P_i^+ is the radiation power transmits to the load from right of the i-th slot; P_i is the radiation power transmits to the load from left of the i-th slot.

According to the equivalent circuit theory [8],[26], the normalized equivalent resistance of the i-th slot can be given as

$$r_i = \frac{E_i^2 q^{-i+1}}{\frac{1}{\eta}\sum_{j=1}^{N} E_j^2 - \sum_{j=1}^{i} E_j^2 q^{-j+1}} \quad (3)$$

Where E_i is the radiating electric magnitude of the i-th slot, η is the radiation efficiency, $q=e^{-2\alpha d}$ is the attenuation and α is the attenuation constant. It can be seen from Eq. (3) that the equivalent resistance of each slot can be obtained by giving the distribution of the radiation field E_i. Additionally, the slot equivalent resistance (r) is related to the slot length (S), the waveguide height (b) and the waveguide width (a), so a needed slot array antenna can be designed by obtaining the relationship between equivalent resistance and the three structural parameters mentioned above, which can be expressed as

$$r = F(S, b, a) \quad (4)$$

III. Design And Simulation Of The Array Antenna

As an example, a leaky-wave array antenna working at 1.57 GHz is designed in this communication. Considering the requirements of practical applications, the antenna parameters are preliminarily selected as follows: θ=30° (From this, the propagation constant can be calculated as $\beta=\beta_0$=16.441 rad/m), w=10 mm, $d=\lambda_g/12$, h=30 mm, the thickness of the waveguide wall is 5 mm and the chamfer radius of the slot edge is 2 mm. The material of the dielectric plate is polypropylene with a relative dielectric constant ε_r=2.2 and a loss tangent tanδ=0.002. The thickness of the dielectric plate is 10 mm.

A. Design and Simulation of Single Waveguide Leaky-Wave Antenna

The impedance of a slot in the periodical circumstance can be obtained by measuring or numerically calculating the S_{21} and S_{11} of the slotted waveguide with M uniform and identical slots [8],[27]. It's worth noting that the slot impedance is the equivalent impedance that includes the mutual coupling. According to the Fig. 2,

$$r_i \approx \frac{P_{ri}}{P_i^+} = \frac{P_i^-}{P_i^+} - 1 = q(\frac{P_i^-}{P_{i+1}^-}) - 1 \quad (5)$$

Ignoring the attenuation, then q=1. If M is large enough that every slot can be seen as identical, then

$$\frac{P_1^-}{P_N} = \frac{P_1^-}{P_2^-}\cdot\frac{P_2^-}{P_3^-}\cdots\frac{P_{N-1}^-}{P_N} = (\frac{P_i^-}{P_{i+1}^-})^N \quad (6)$$

Then, we have

$$r_i = \left(\frac{P_1^-}{P_L}\right)^{\frac{1}{N}} - 1 = \xi^{-\frac{1}{N}} - 1 \quad (7)$$

$$\xi = \frac{|S_{21}|^2}{1-|S_{11}|^2} \quad (8)$$

So, we can get:

$$r = \left(\frac{|S_{21}|^2}{1-|S_{11}|^2}\right)^{-\frac{1}{M}} - 1 \quad (9)$$

According to Eq.(9), the relationship of the slot equivalent resistance and the slot length S, the waveguide height b, the waveguide width a can be obtained by calculating the S_{11} and S_{21} of the slotted waveguide with M identical slots. Fig. 3(a) shows the relationship between the slot length (S) and the equivalent resistance (r) when the waveguide height (b) is 70 mm. Significantly, the waveguide width (a) is also changed with S and r correspondingly to counteract the extra phase delay caused by the non-resonant slots, thus keeping the propagation constant unchanged. Therefore, Fig. 3(b) shows the relationship between a and r when b is 70 mm. As can be seen from Fig. 3(a, b), the maximum normalized resistance (r) is less than 0.12. However, according to the aperture distribution curve (Fig.4), which will be discussed later in this communication, a normalized resistance of 0.12 is still not enough to realize the desired aperture distribution. If S increases further, the increase in normalized resistance is not obvious and a large reflection will be induced. Therefore, we change another structural parameter (the waveguide height b) to increase r while keeping S at 77mm. Fig. 3(c) shows the relationship between b and r when the slot length (S) is 77 mm. It can be seen from it that the maximum value of the normalized resistance exceeds 0.14, which satisfies the requirement of the aperture distribution. Similarly, the waveguide width (*a*) is also changed with *b* correspondingly to counteract the extra phase delay caused by the non-resonant slots, thus keeping the guided wavelength unchanged. Fig. 3(d) illustrates the relationship between *a* and *r* when *S* is 77 mm. The data fitting formulas are expressed by Eq. (10) and Eq. (11) respectively.

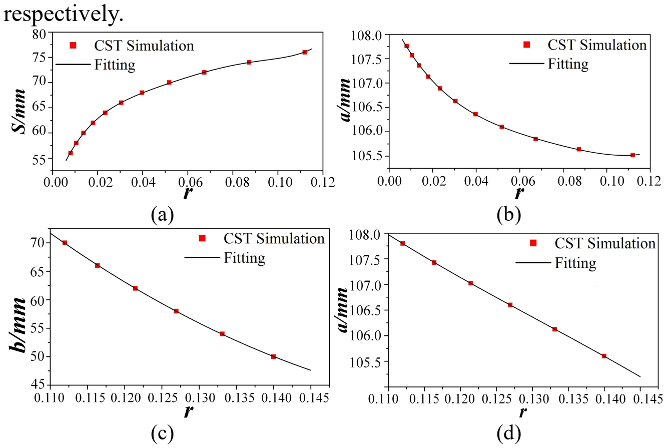

Fig. 3. Structural parameters versus the equivalent resistance. (a,b) *b*=70 mm. (c,d) *S*=77 mm.

$$\begin{cases} S = 0.0484 + 1.1972r - 32.4495r^2 + 507.5615r^3 \\ \quad -3954.8671r^4 + 11908.188r^5 \\ a = 0.1084 - 0.0926r + 1.4559r^2 - 12.3192r^3 - 41.5037r^4 \\ b = 70 \end{cases} \tag{10}$$

$$\begin{cases} b = 0.2557 - 2.4197r + 6.7879r^2 \\ a = 0.1177 - 0.2326r + 1.5458r^2 - 3.9381r^3 \\ S = 77 \end{cases} \tag{11}$$

Considering power-handling capacity, antenna efficiency and the range of the equivalent resistance, we choose a combined aperture field distribution to design the antenna, as shown in Fig. 4. The radiation efficiency of the antenna is set to be 97%. Then, the equivalent resistance of each slot can be calculated by the aperture field distribution using Eq.(3). The total number of slots is 66. The first 25 slots and the last 33 slots are corresponding to the front and back parts of two parabola distribution functions. The 8 slots in the middle adopt a uniform distribution. By this means, the electric field amplitudes corresponding to the first 25 slots are larger, which means that more energy can be radiated. Thus, the maximum electric field amplitude of the middle slots can be reduced and the power-handling capacity of the antenna would also be improved due to the uniform distribution. The parabolic parameter in the back section is small, which can effectively reduce the value of the maximum equivalent resistance.

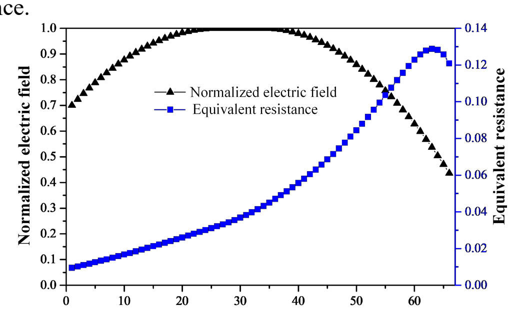

Fig. 4. Aperture distribution of the antenna and the equivalent resistance of each slot.

Combining Eq.(10), (11) and the resistance distribution shown in Fig. 4, we can get the length of each slot and the corresponding waveguide width and height, as shown in Fig. 5. The height of the waveguide (*b*) corresponding to the first 57 slots is kept at 70 mm and the length of the final 9 slots (*S*) is kept at 77 mm. The total length of the single waveguide leaky-wave antenna is 2.39 m.

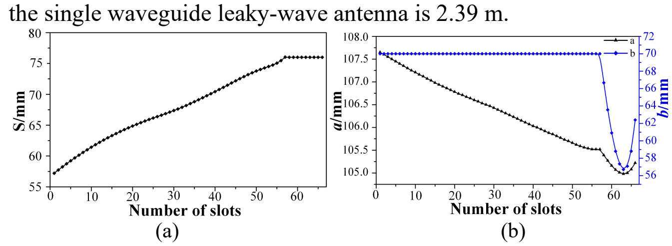

Fig. 5. (a) Length of each slot. (b) Waveguide width and height corresponding to each slot.

The simulated electric field distribution in the antenna is shown in Fig. 6. It can be seen clearly from Fig. 6(a) that the wave propagates in traveling state and most of the power is radiated. No electric field enhancement appears on the slots, which means that the power-handling capacity of the waveguide does not diminish. The maximum electric field strength in the waveguide is 1.23 kV/m when the input power is 0.5 W. According to Ref.[20], the electric field breakdown threshold of the metal can be 70 MV/m under the vacuum condition, it can be obtained that a single slotted waveguide has a power-handling capacity of 1.63 GW. The maximum electric field strength is 69 V/m on the dielectric plate surface and the electric field breakdown threshold of the dielectric can reach 4 MV/m under the vacuum condition, so the dielectric cover has a power-handling capacity of 1.68 GW. In general, the power-handling capacity of a single waveguide leaky-wave antenna is about 1.63 GW.

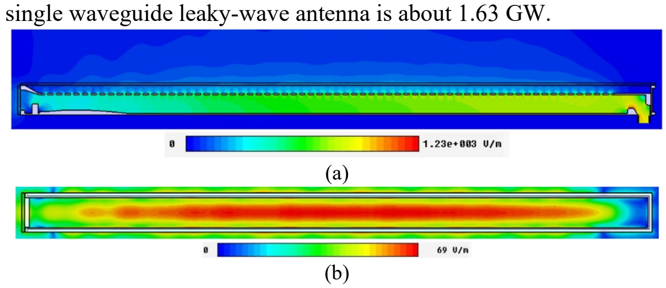

Fig. 6. (a) Electric field distribution inside the slotted waveguide. (b) Electric field distribution on the dielectric plate surface.

Fig. 7 shows the reflection coefficient of the antenna. At the central frequency, the reflection is less than -30 dB. Over the frequency range of 1.53~1.62 GHz, the reflection is below -20 dB, the relative bandwidth of the antenna is about 5.73%. The simulated single antenna model includes an output port, which will contain an absorber to absorb the remaining energy in practical use. Thus, the S_{21} parameter of the antenna is also shown in Fig. 8, which is -15.34 dB at the central frequency. Therefore, it can be calculated that the radiation efficiency of the antenna is 97.1% at the central frequency, which is consistent with the theoretical design results.

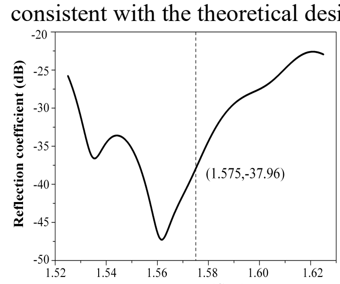

Fig. 7. Reflection coefficient of the antenna.

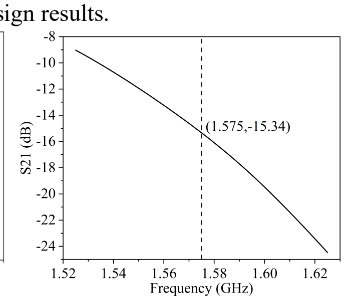

Fig. 8. S_{21} parameter of the antenna.

Fig. 9 gives the far-field radiation pattern of the antenna. The main lobe gain of the slotted waveguide antenna is 17.9 dB with a 29.7° deflection in elevation plane. The half-power beam width (HPBW) of the *E*-plane and *H*-plane are 5.8° and 120°, respectively. When setting several waveguides to an array along the *H*-plane, the gain and power-handling capacity of the antenna would be further improved.

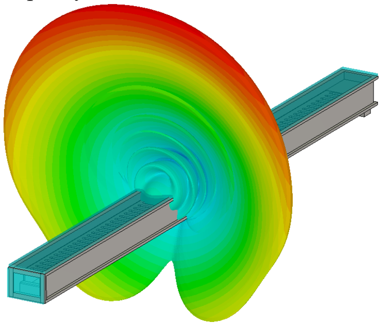

Fig. 9. Simulated 3-D radiation pattern of the single antenna.

B. Design and Simulation of Slotted Waveguide Array

In this section, the proposed single-waveguide antenna is fully employed to construct a 5-waveguide array. As seen in Fig. 1(a), the first and the fifth waveguides are symmetrical about the median plane of the array, the second and the fourth waveguides are symmetrical about the median plane of the array. Therefore, the boundary conditions of the first, second and third waveguides are different from each other. Considering the mutual coupling between the waveguides, it is necessary to establish an electric parameters extraction model including five waveguides, and extract the electric parameters of the first, the second and the third waveguide slots, respectively. The propagation constant in the waveguides should keep at β_0 during electric parameters extraction. After extracting the electric parameters, we also use the aperture distribution function shown in Fig. 4 to design the slots array. Fig. 10 shows the 3-D radiation pattern of the slots array when the five waveguides are excited with equal power and the same phase. The gain of the array is 25 dB with an aperture efficiency of 76.6%. Combining with the high-power phase-shifter [22],[23], the phases of the inject wave between adjacent waveguides can be sequentially different by $\Delta\varphi$, the array antenna can steer the beam in H-plane, as seen in Fig. 11 and Fig. 12. The beam scanning range of the array is ±40°. As the beam scanning angle increases, the gain gradually decreases from 25 to 23.3 dB and the gain variation is less than 2 dB. During beam scanning, the side lobe of the array antenna does not increase significantly, indicating a good performance of the array antenna.

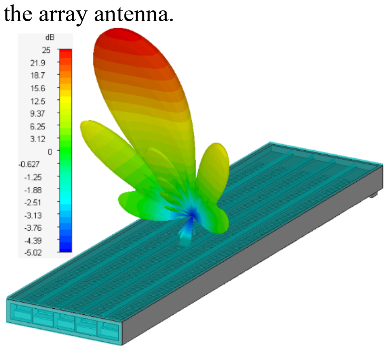

Fig. 10. Simulated 3-D radiation pattern of the array antenna.

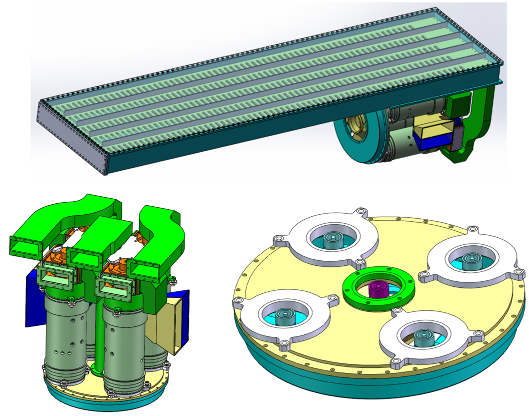

Fig. 11. High-power phase-shifter.

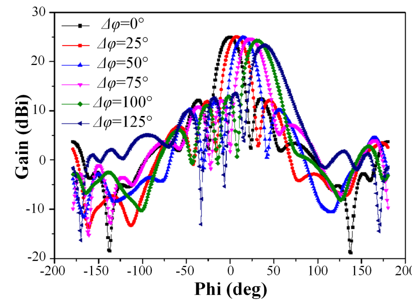

Fig. 12. Simulated radiation pattern of the array antenna.

IV. Experiment Results

A. Lower Power Test

To verify the feasibility of the design method we proposed, a prototype was fabricated, as shown in Fig. 13. The antenna was measured in the anechoic chamber. A mode converter and a transitional rectangular waveguide are used between the leaky-wave antenna and the VNA. The receiving antenna is covered with absorbing turf to reduce microwave reflection, thus ensuring the accuracy of the measurement. The photographs are shown in Fig. 14. The results of the antenna reflection coefficient are shown in Fig. 15. The experimental results are consistent with the simulation results, and the difference between them is mainly caused by the systematic error which comes from the connection between the waveguide and the vector network analyzer.

(a)

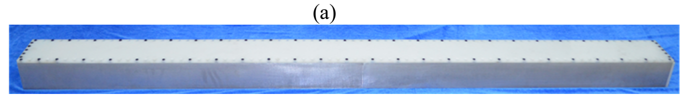

(b)

Fig. 13. Photograph of the leaky-wave antenna. (a) Without dielectric cover. (b) With dielectric cover.

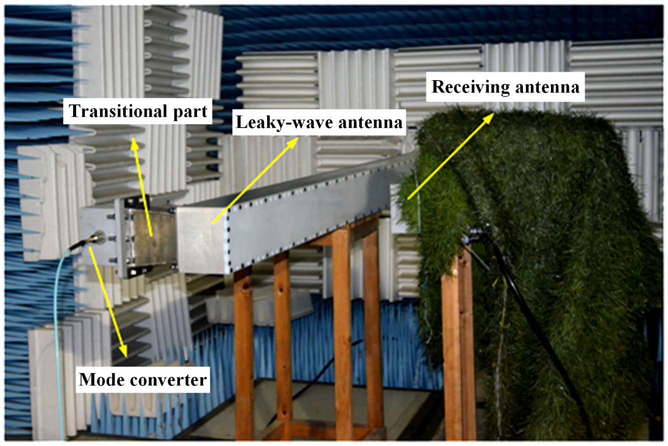

Fig. 14. Measurement of the leaky-wave antenna.

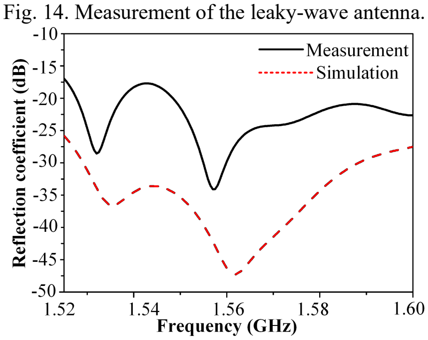

Fig. 15. Measured reflection coefficient of the leaky-wave antenna.

The measured radiation patterns at 1.57 GHz are shown in Fig. 16, which agree well with the simulation results. It is clear from the figure that the antenna is a linearly polarized antenna and the cross-polarization component is mainly on the H-plane.

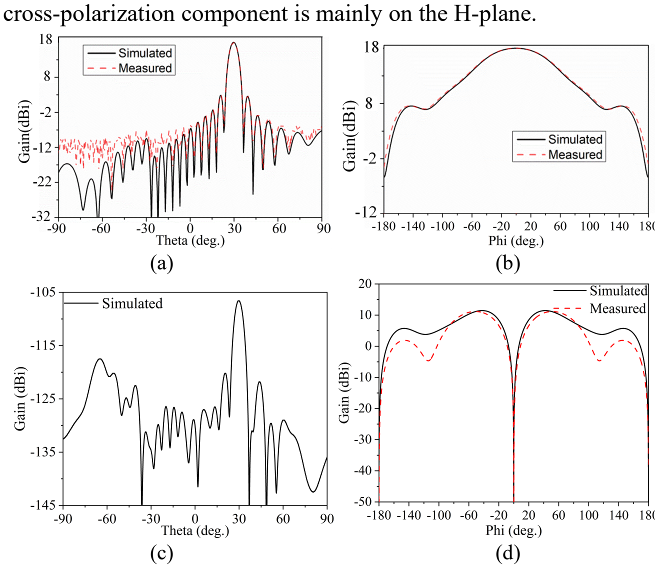

Fig. 16. (a) Co-polar radiation pattern on E-plane. (b) Co-polar radiation pattern on H-plane. (c) Cross-polar radiation pattern on E-plane. (d) Cross-polar radiation pattern on H-plane.

B. High Power Test

To identify the power-handling capacity of the leaky-wave antenna, high power experiments have been developed. The entire structure was studied on the HPM system of an L-band magnetically insulated transmission-line oscillator (MILO) [19], as shown in Fig. 17. The MILO produced an HPM pulse at 1.57 GHz, 1.2-2 GW, and for 52ns. The output mode of the MILO is TM_{01} mode and firstly converted into rectangular TE_{10} mode by a circular-rectangular mode converter designed by our laboratory [28]. After that, the TE_{10} mode is fed into the leaky-wave antenna. For accuracy, five receiving horns are set at different angles (26°, 28°, 30°, 32° and 34°) to measure the radiation power synchronously. The typical waveforms of the radiation pulses at power 1.3 GW detected are illustrated in Fig. 18(a). As illustrated, the pulse duration of all obtained waveforms is over 51 ns. No grievous breakdown or pulse shortening occurred in the experiments. The typical waveforms of the radiation pulses at power 1.5 GW detected are illustrated in Fig. 18(b). Some of the obtained pulse duration is less than 50 ns, which means that electric breakdown has occurred at some positions in the antenna. Therefore, the power-handling capacity of the single leaky-wave antenna is greater than 1.3 GW and less than 1.5 GW.

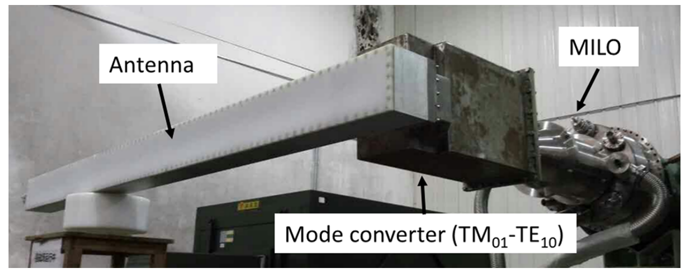

Fig. 17. Device of high-power experiment.

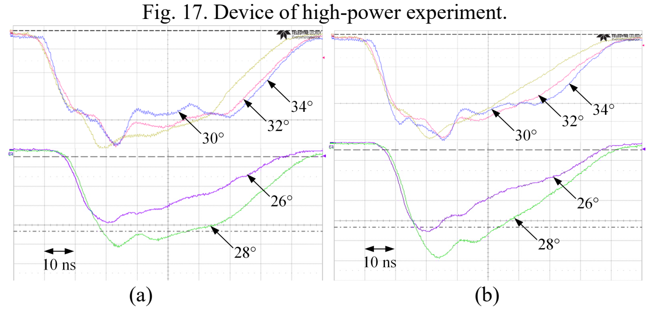

Fig. 18. Detected microwave of the HPM source. (a) Radiation power is1.3 GW. (b) Radiation power is 1.5 GW.

V. Conclusion

In this communication, a design method of leaky-wave antenna based on rectangular waveguide with transverse slots is presented. A single waveguide leaky-wave antenna and a planar array composed of five waveguides have been designed. Moreover, the experimental study of a single waveguide leaky-wave antenna was carried out. Experimental results show that the proposed antenna has a high power-handling capacity and a compact structure. The simulation results show that the aperture efficiency of the whole array exceeds 76.6% and beam scanning range can reach ±40° in *H*-plane. It also provides a new way to design compact high-power microwave antenna.

References

[1] S. R. Rengarajan, L. G. Josefsson, and R. S. Elliott, "Waveguide-fed slot antennas and arrays: A review," *Electromagnetics,* vol. 19, no. 1, pp. 3-22, 1999.

[2] R. Petersson, E. Kallas, and K. Van't Klooster, "Radiation performance of the ERS-1 SAR EM antenna," in *1988 IEEE AP-S. International Symposium, Antennas and Propagation*, 1988: IEEE, pp. 212-215.

[3] R. E. Cowdery and W. A. Skillman, "Development of the airborne warning and control system (AWACS) radar," *IEEE Transactions on Aerospace and Electronic Systems,* vol. 31, no. 4, pp. 1357-1365, 1995.

[4] W. Coburn, M. Litz, J. Miletta, N. Tesny, L. Dilks, and B. King, "A slotted-waveguide array for high-power microwave transmission," Army Research Lab Adelphi MD, 2001.

[5] N. R. Devarapalli, C. E. Baum, C. G. Christodoulou, and E. Schamiloglu, "A Fan-Beam Radiator Using Waveguide's Narrow Wall for Horizontal Polarization and High Power," *IEEE transactions on electromagnetic compatibility,* vol. 53, no. 2, pp. 380-389, 2011.

[6] X. Pan and C. G. Christodoulou, "A narrow-wall slotted waveguide antenna array for high power applications," in *2014 IEEE Antennas and Propagation Society International Symposium (APSURSI)*, 2014: IEEE, pp. 1493-1494.

[7] L. Yu, C. Yuan, J. He, and Q. Zhang, "Beam Steerable Array Antenna Based on Rectangular Waveguide for High-Power Microwave Applications," *IEEE Trans. Plasma Sci.,* vol. 47, no. 1, pp. 535-541, 2019, doi: 10.1109/TPS.2018.2884290.

[8] Y. Yang, C. Yuan, and B. Qian, "A beam steering antenna for X-band high power applications," *AEU-International Journal of Electronics and Communications,* vol. 68, no. 8, pp. 763-766, 2014.

[9] J. D. Binion *et al.*, "A Slotted Waveguide Antenna Array for High-power Microwave Applications," in *2020 IEEE International Symposium on Antennas and Propagation and North American Radio Science Meeting*, 5-10 July 2020 2020, pp. 231-232, doi: 10.1109/IEEECONF35879.2020.9330128.

[10] R. Meng, Y. Xia, Y. Guo, and Q. Zhu, "An X-Band 48-Way Leaky Waveguide Antenna With High Aperture Efficiency and High Power Capacity," *IEEE Trans. Antennas Propag.,* vol. 66, no. 12, pp. 6799-6809, 2018.

[11] L. Guo, W. Huang, C. Chang, J. Li, Y. Liu, and R. Meng, "Studies of a Leaky-Wave Phased Array Antenna for High-Power Microwave Applications," *IEEE Trans. Plasma Sci.,* vol. 44, no. 10, pp. 2366-2375, 2016, doi: 10.1109/TPS.2016.2601105.

[12] F. Frezza, M. Guglielmi, and P. Lampariello, "Millimetre-wave leaky-wave antennas based on slitted asymmetric ridge waveguides," *IEE Proceedings - Microwaves, Antennas and Propagation*, vol. 141, no. 3, pp. 175-180. [Online]. Available: https://digital-library.theiet.org/content/journals/10.1049/ip-map_19941006

[13] C. D. I. Nallo, F. Frezza, A. Galli, G. Gerosa, and P. Lampariello, "Stepped leaky-wave antennas for microwave and millimeter wave applications," *Annales Des Télécommunications,* vol. 52, no. 3, pp. 202-208, 1997/03/01 1997, doi: 10.1007/BF02996045.

[14] J. Liu, D. R. Jackson, and Y. Long, "Substrate integrated waveguide (SIW) leaky-wave antenna with transverse slots," *IEEE Trans. Antennas Propag.,* vol. 60, no. 1, pp. 20-29, 2011.

[15] J. Liu, X. Tang, Y. Li, and Y. Long, "Substrate integrated waveguide leaky-wave antenna with H-shaped slots," *IEEE Trans. Antennas Propag.,* vol. 60, no. 8, pp. 3962-3967, 2012.

[16] X. Zou, D. Yu, Y. Fan, J. Li, and W. Luo, "A Substrate-Integrated Waveguide Leaky-Wave Antenna Based on Eye-Shaped Transverse Slot," *IEEE Trans. Antennas Propag.,* vol. 69, no. 11, pp. 7947-7952, 2021.

[17] D. Zheng, Y. L. Lyu, and K. Wu, "Longitudinally Slotted SIW Leaky-Wave Antenna for Low Cross-Polarization Millimeter-Wave Applications," *IEEE Trans. Antennas Propag.,* vol. 68, no. 2, pp. 656-664, 2020, doi: 10.1109/TAP.2019.2940469.

[18] C. Chang, G. Liu, C. Tang, C. Chen, and J. Fang, "Review of recent theories and experiments for improving high-power microwave window breakdown thresholds," *Physics of Plasmas,* vol. 18, no. 5, p. 055702, 2011.

[19] Y.-W. Fan, X.-Y. Wang, H.-H. Zhong, and J.-D. Zhang, "A dielectric-filled magnetically insulated transmission line oscillator," *Appl. Phys. Lett.,* vol. 106, no. 9, p. 093501, 2015.

[20] V. Dolgashev, S. Tantawi, Y. Higashi, and B. Spataro, "Geometric dependence of radio-frequency breakdown in normal conducting accelerating structures," *Appl. Phys. Lett.,* vol. 97, no. 17, p. 171501, 2010.

[21] L. Goldstone and A. Oliner, "Leaky-wave antennas I: Rectangular waveguides," *IRE Transactions on Antennas and Propagation,* vol. 7, no. 4, pp. 307-319, 1959, doi: 10.1109/TAP.1959.1144702.

[22] Q. Zhang, C. Yuan, and L. Liu, "Studies on mechanical tunable waveguide phase shifters for phased-array antenna applications," in *2016 IEEE International Symposium on Phased Array Systems and Technology (PAST)*, 2016: IEEE, pp. 1-3.

[23] Y.-M. Yang, C.-W. Yuan, and B.-L. Qian, "A novel phase shifter for Ku-band high-power microwave applications," *IEEE Trans. Plasma Sci.,* vol. 42, no. 1, pp. 51-54, 2013.

[24] G. Stern and R. Elliott, "Resonant length of longitudinal slots and validity of circuit representation: Theory and experiment," *IEEE Trans. Antennas Propag.,* vol. 33, no. 11, pp. 1264-1271, 1985, doi: 10.1109/TAP.1985.1143509.

[25] A. F. Stevenson, "Theory of Slots in Rectangular Wave-Guides," *J. Appl. Phys.,* vol. 19, no. 1, pp. 24-38, 1948, doi: 10.1063/1.1697868.

[26] R. Elliott, "An improved design procedure for small arrays of shunt slots," *IEEE Trans. Antennas Propag.,* vol. 31, no. 1, pp. 48-53, 1983, doi: 10.1109/TAP.1983.1143002.

[27] L. Teng, H. Meng, and W. Dou, "Design and Implementation of Dual-Frequency Dual-Polarization Slotted Waveguide Antenna Array for Ka-Band Application," *IEEE Antennas & Wireless Propagation Letters,* vol. 13, pp. 1317-1320, 2014.

[28] X. Zhao, C. Yuan, Z. Qiang, and L. Zhao, "Design and experiment study of compact circular-rectangular waveguide mode converter," *Rev. Sci. Instrum.,* vol. 87, no. 7, p. 074707, 2016.